Joining of CVD-SiC coated and uncoated fibre reinforced ceramic matrix composites with pre-sintered Ti_3SiC_2 MAX phase using Spark Plasma Sintering

[*] Peter Tatarko[a], Valentina Casalegno[b], Chunfeng Hu[c], Milena Salvo[b], Monica Ferraris[b], [†]Michael J. Reece[a],

[a]School of Engineering & Materials Science and Nanoforce Technology Ltd., Queen Mary University of London, Mile End Road, London E1 4NS, United Kingdom

[b]Politecnico di Torino, Department of Applied Science and Technology, Corso Duca degli Abruzzi 24, 10129 Torino, Italy

[c]Key Laboratory of Advanced Technologies of Materials, Ministry of Education, School of Materials Science and Engineering, Southwest Jiaotong University, Chengdu, Sichuan 610031, China

Abstract

CVD-SiC coated and uncoated ceramic matrix composites were successfully joined to their counterparts with a pre-sintered Ti_3SiC_2 foil using Spark Plasma Sintering. For the first time pre-sintered Ti_3SiC_2 foil was used as a joining filler. The joining parameters were carefully selected to avoid the decomposition of Ti_3SiC_2 and the reaction between the joining filler and the CVD-SiC coating, which would have deteriorated the oxidation protective function of the coating. Conformal

[*] Corresponding authors: p.tatarko@nanoforce.co.uk
[†]   m.j.reece@qmul.ac.uk

behaviour of the Ti$_3$SiC$_2$ foil during the diffusion joining and the infiltration of the joining filler into the surface cracks in the CVD β-SiC coating allowed filler to be more integrated with the matrix material. While diffusion bonding occurred during joining of the coated composites, a combination of both reaction and diffusion bonding was observed for the uncoated C$_f$/SiC composites. This produced the lower shear strength (19.1 MPa) when compared to the diffusion bonded CVD-SiC coated C$_f$/SiC strength (31.1 MPa).

Keywords: ceramic matrix composites; joining; MAX phase; CVD-SiC coating; Spark Plasma Sintering

1. Introduction

Advanced ceramic matrix composites (CMCs) based on a SiC matrix reinforced either with carbon fibres (C$_f$/SiC) or silicon carbide fibres (SiC$_f$/SiC) are materials of great interest for aerospace [1, 2, 3] and nuclear applications [4, 5, 6] due to their superior mechanical properties, resistance against high temperatures and their light weight. CMCs typically consist of straight or woven ceramic fibres embedded in a ceramic matrix with a weak bond between them resulting in the improved fracture toughness of the materials [7]. They are being used as thermo-structural materials in different fields, such as components of heat exchangers, gas turbines for power plants, heat shields for space vehicles (thermal protection system), inner wall of plasma chamber of nuclear fusion reactors, aircraft brakes, body flaps, leading edges, heat treatment furnaces, etc. [1, 2]. Since the CMCs are used for applications operating at very high temperatures, they are usually coated with an outer CVD-SiC protective layer to improve their oxidation and ablation

resistance [2]. In many cases, however, their application will depend on the ability to join them because the manufacture of these materials as large components with complicated shapes is extremely difficult and expensive. A critical issue of the wider use of CMCs is thus the development of inexpensive, reliable and user-friendly joining methods to assemble them as large components in complex structures [1].

In recent years, Spark Plasma Sintering (SPS, also referred to as field-assisted sintering technology (FAST)) has attracted considerable interest as a new advanced technique for joining of both monolithic SiC [8, 9, 10] and CMC materials [1, 9, 11]. In this case, both a rapid heating and a short processing time allow a highly controllable reaction of the interlayer with the materials to be joined. At the same time, the electric field can accelerate self-diffusion, and promote the migration of ions through the joining interface [10].

In order to develop new techniques to join advanced CMC materials that can perform in extreme environments, a critical issue is to develop new filler materials with high melting points and good oxidation resistance. A family of layered ternary materials, so-called "MAX" phases ($M_{n+1}AX_n$, where n is 1, 2 or 3, M is an early transition metal, A is an A-group element, and X is either C or N) have attracted increasing attention during the last decade. MAX phases exhibit a unique combination of metallic and ceramic properties, such as damage tolerance, machinability, high temperature oxidation resistance, good electrical and thermal conductivities, thermal shock resistance, and wear resistance [12]. Moreover, they exhibit large plastic deformation at temperatures above 1300°C [13, 14]. Since MAX phases also possess excellent irradiation/corrosion resistance, they are regarded as promising structural materials for fusion reactors and lead-cooled fast reactors [15].

Among all of the MAX phase materials, Ti_3SiC_2 has been considered the most promising candidate structural material for nuclear and high-temperature applications [10]. More recently, Ti_3SiC_2 has attracted considerable attention as a joining filler for SiC [8, 9, 10] and CMC materials [9, 11].

Dong et al. [9] used a pre-synthesized Ti_3SiC_2 powder (containing ~ 10 vol.% of TiC) to join both SiC and C_f/SiC materials using hot-pressing technology at different temperatures from 1300°C to 1600°C with a dwell time of 30 minutes. The flexural strength of the joints increased with increasing joining temperature and reached a maximum value of ~ 110 MPa for SiC joined at 1600°C. However, at the same time, the amount of Ti_3SiC_2 decreased with increasing joining temperature, while the amount of TiC and $TiSi_2$ increased due to chemical reaction and decomposition of Ti_3SiC_2. On the other hand, no chemical reaction took place at a joining temperature of 1300°C, but the lowest flexural strength was measured. Zhou et al. [10] joined pressureless sintered SiC with a Ti_3SiC_2 tape film (made using a commercial Ti_3SiC_2 powder) using SPS at temperatures from 1300°C to 1600°C with a dwell time of 5 minutes. Similar to the previous work, flexural strength increased with increasing joining temperature and reached a maximum value of ~ 99 MPa at a joining temperature of 1500°C. Again, they suggested that interface reactions were beneficial for achieving a higher joining strength. In recent work, a Ti_3SiC_2 tape was also used to join C_f/C composites using SPS processing at temperatures between 1100°C and 1400°C [11]. A relatively high shear strength (~ 26 MPa) was measured for the components joined at 1200°C and 1300°C. This was attributed to the strong bonding between the interlayer and the matrix resulting from the reaction between them. The reaction was the result of a partial decomposition of Ti_3SiC_2, followed by

a reaction with carbon from the C_f/C matrix to form SiC and cubic TiC at the interface. The shear strength significantly dropped when the joining temperature was 1400°C due to almost complete decomposition of Ti_3SiC_2.

In all these works, the joining procedures relied on the reaction between the joining filler and the matrix to obtain a good strength of the joined components. However, decomposition of Ti_3SiC_2 occurring at the joining temperatures along with the chemical reactions with the matrices led to a decreasing amount of Ti_3SiC_2 in the joining area. In other words, although the Ti_3SiC_2 powders were used to join SiC and CMC materials, the best results were achieved when the amount of Ti_3SiC_2 used decreased due to both its partial decomposition and chemical reaction with SiC and C. It should also be pointed out that this reaction could cause damage to the SiC oxidation protective outer layer on the CMCs.

Although CMC materials are usually covered by a CVD-SiC oxidation protective coating for their final applications, to the best of the authors' knowledge, there has been no reported study on the joining of CVD-SiC coated CMCs with Ti_3SiC_2 MAX phase. Therefore, the aim of the present work was to develop a technique to join SiC_f/SiC and C_f/SiC composites, both coated with an oxidation protective layer of CVD β-SiC. In order to conduct a systematic study, two uncoated C_f/SiC composites with different types of carbon fibres were also joined using the same technique for the sake of comparison. Unlike the synthesized Ti_3SiC_2 powder [9] or Ti_3SiC_2 tapes [10, 11], this is the first report of using pre-sintered Ti_3SiC_2 to join CMC materials via solid-state diffusion bonding. The Ti_3SiC_2 foil was pre-sintered from a synthesized Ti_3SiC_2 powder [16] (containing a small amount of impurities in the form of TiC and Ti_5Si_3) using SPS and then ground down to 80 - 100 μm thickness.

After the SPS sintering, the amount of impurities (TiC and Ti_5Si_3) was negligible and the Ti_3SiC_2 foil containing $\sim$ 4.8 wt.% Al_2O_3 was used as a joining filler. The addition of Al for the synthesis of Ti_3SiC_2 was reported to significantly decrease the quantity of the TiC impurity [16] as well as to improve the oxidation resistance of Ti_3SiC_2 [17]. Similarly, the presence of Al_2O_3 in the final synthesized Ti_3SiC_2 powder should improve the hardness, strength and fracture toughness of Ti_3SiC_2 material [16]. The advantages of using pre-sintered foil rather than powder and/or tape lie in the fact that due to the solid-state diffusion bonding (no melting of joining material) there is neither densification nor reaction required to obtain sound joints. This should rule out the possibility of undesirable shrinkage of the joining interlayer as well as its reaction with the CVD-SiC coated CMCs. Any reaction between the filler and the matrix could cause damage to the external CVD β-SiC layer, which would deteriorate the oxidation protective function of the coating. Therefore, the joining parameters were carefully chosen to avoid decomposition of Ti_3SiC_2 and the reactions between the joining filler and CVD coating. Using such an approach, sound joints with a high joining strength were obtained by diffusion bonding using SPS at a temperature as low as 1300°C, with an external pressure of 50 MPa and a dwell time of 5 minutes.

2. Experimental procedure

2.1 Materials to be joined

Four different CMCs (all supplied by MT Aerospace, Germany) were joined with the Ti_3SiC_2 pre-sintered foil using the SPS. All samples were manufactured at MT Aerospace using the standard gradient Chemical Vapour Infiltration (CVI) process and supplied as rectangular shaped samples. As-received CMCs materials

are summarized in Table 1. All of the CMCs materials contained characteristic natural flaws, such as macro pores between the individual fabric layers or surface cracks in the CVD β-SiC layer; see the supplementary material, S.1.

Table 1 List of as-received CMC materials to be joined

Material	Fibres	Surface finish	Density [g/cm³]	Dimension [mm]
SiC_f/SiC	Tyranno® S grade 1.6 K (Ube Industries, ltd.)	coated by CVD β-SiC	2.4	10 x 10 x 3
C_f/SiC	T300 1K (Torayca®)	coated by CVD β-SiC	2.0	10 x 10 x 3
C_f/SiC	T300 1K (Torayca®)	uncoated	1.8	10 x 9 x 3
C_f/SiC	M40J 3K (Torayca®)	uncoated	1.8	10 x 7 x 3

Besides Keraman® SiC_f/SiC and C_f/SiC samples coated with a protective CVD β-SiC layer, two uncoated C_f/SiC ceramic composites were joined and investigated with two main aims: i) to investigate the influence of a SiC coating on the joining process as well as the mechanical performance of the joints; ii) to investigate the influence of different carbon fibres on the joining process and mechanical performance of the joined components. Regarding the second point, the main difference between the carbon fibres is their different stiffness's. According to the supplier, the M40J 3K carbon fibres (tensile modulus of ~ 230 GPa) are much stiffer than the T300 1K ones (tensile modulus of ~ 135 GPa). The stiffer carbon fibres led to a greater separation of the individual fabric layers in the initial CMC materials, see the Figure S.1 in the supplementary material.

2.2 Material for joining filler

Details about the synthesis of the Ti_3SiC_2 powder used in this work and its characterisation are reported elsewhere [16]. Briefly, the powder was synthesized

from the elemental powders in the molar ratio of 1.0 Ti / 1.2 Si / 0.3 Al / 2.0 TiC in flowing argon at 1200°C for 2 hours using in tungsten furnace. This powder was sintered using SPS at a temperature of 1300°C with an external pressure of 50 MPa and a dwell time of 5 minutes in vacuum. The as-sintered Ti_3SiC_2 bulk samples were then ground and polished using a final diamond suspension of 3 μm to produce the thin foils with a final thickness of 80 - 100 μm. Afterwards, the pre-sintered foils were cut into a rectangular shape to match the dimensions of the cross section of the CMCs and then used as a joining filler.

2.3 SPS joining process

The CMC materials were always joined to a counterpart made of the same CMC. Before joining, the CMCs as well as the Ti_3SiC_2 pre-sintered foils were ultrasonically cleaned in acetone. A sketch of the j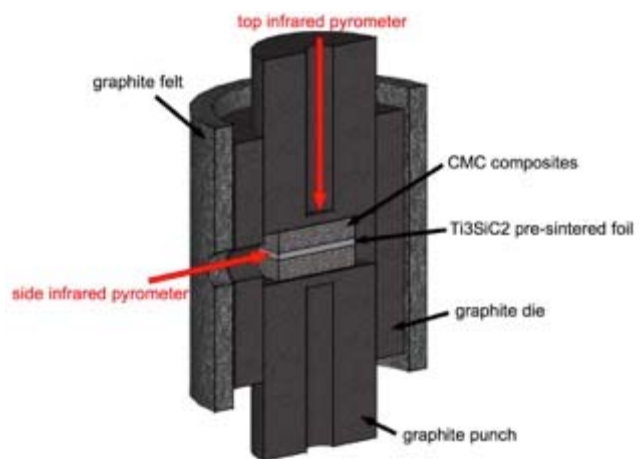oining setup is shown in Fig. 1. The Ti_3SiC_2 foil was interposed between two CMC samples as a sandwich and inserted into a cylindrical

Fig. 1 Sketch of the joining setup for the SPS process.

graphite die with a diameter of 20 mm. The external pressure was applied through the graphite punches inserted in the cylindrical die. The graphite die was then wrapped in graphite felt, and both the die and the felt had a small hole enabling the temperature at the joining interface to be measured via a side-viewing infrared pyrometer. The joining assembly was heated to the joining temperature indirectly by Joule heating of the graphite die, which was heated by pulsed electric current in

vacuum in an SPS furnace (HPD 25/1, FCT systems, Germany). The joining temperature was controlled using a top-viewing infrared pyrometer (measuring the temperature at ∼ 2 mm from the top surface of the sample) while monitoring the temperature of the joining interface using the side-viewing optical pyrometer (see Fig. 1). The temperature difference measured using the top and side pyrometers was negligible (les than 5°C) due to a relatively small height of the whole assembly (∼ 6 mm) and uniform indirect heating via the graphite die. Therefore the joining temperature referred hereinafter is that measured by the top pyrometer. The joining temperature was 1300°C and the external pressure was 50 MPa. The heating and cooling rates were 100°C/min while the holding time at the maximum temperature was 5 minutes.

2.4 Materials characterisation

The mechanical strength of the joined samples was evaluated using a single lap offset shear test. The tests were performed using a compression testing machine (SINTEC D/10) at room temperature, according to a method adapted from standard ASTM D1002-05. Before testing, Cu bars were placed on the opposite sides of the joined assembly as an artificial step to enable the single lap offset configuration (Fig. 2). A shear load was applied by moving the cross-head at a speed of 0.5 mm/min. The maximum force was recorded and the apparent shear strength was calculated by dividing the maximum force by the joining area (∼ 100 m^2). At least 3 samples of each joined material were tested.
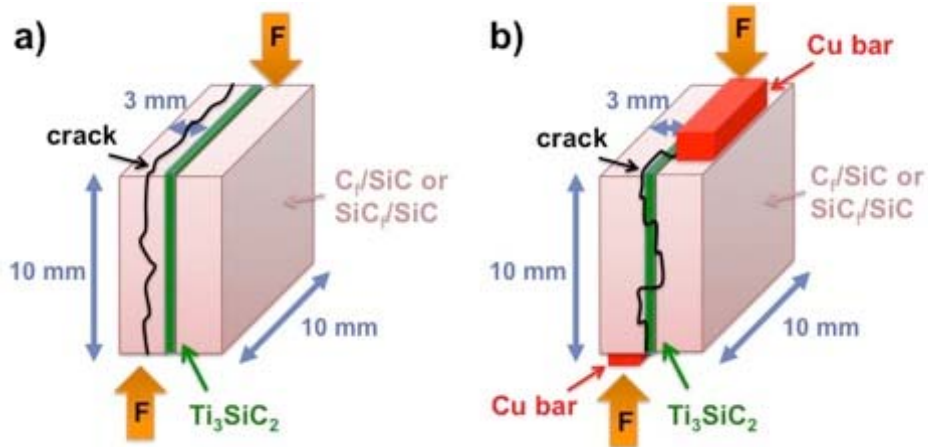
Fig. 2 A schematic illustration of the mechanical testing of the joined components; a) single lap shear test; b) single lap offset shear test.

X-ray diffraction (XRD) patterns of both the Ti_3SiC_2 powder and the Ti_3SiC_2 bulk samples were obtained with an X-ray diffractometer (Siemens D5000 using Cu Kα radiation). Micro-XRD of the fracture surfaces of the samples after the single lap offset shear tests was performed using a Rigaku D/max-Rapid Microdiffractometer (The Woodlands, USA) with collimator spot area of 300 μm. The CMCs before joining, polished cross-sections of the joining areas and fracture surfaces after the mechanical tests were characterized using Scanning Electron Microscopy (SEM) FEI Inspect-F equipped with Energy Dispersive Spectroscopy (EDS) detector.

3. Results and discussion

3.1 SPS sintering of the Ti_3SiC_2 powder

The as-synthesized powder contained the main Ti_3SiC_2 phase, a small amount of impurities (< 10 vol.%), such as TiC and Ti_5Si_3, then intentionally added Al_2O_3 (~ 4.8 wt.%; ~ 7.1 mol.%), and a small amount of both Al (~ 1.3 wt.%; ~ 7.15 mol.%) and Si (~ 2.6 wt.%; ~ 14.4 mol.%) [16]. The details about the synthesis of the Ti_3SiC_2 were reported elsewhere [16]. The SPS sintering process at such a low

temperature (1300°C) and a short time (5 minutes) purified the as-synthesized powder and the amount of the impurities (TiC and Ti_5Si_3) was negligible after the SPS sintering, see the supplementary material, S.2. Therefore the as-sintered material, containing Al_2O_3 and a small amount of Al and Si, was further ground down to a final thickness between 80 and 100 µm and then used as a joining foil between pairs of CMCs. The details about the SPS sintering of the as-synthesized Ti_3SiC_2 powder along with the XRD patterns of both the as-synthesized Ti_3SiC_2 powder and the bulk Ti_3SiC_2 sample after SPS sintering are given in the supplementary material, Figure S.2.

3.2 Cross-section analysis of the joined CMCs coated with protective CVD β-SiC layer

The CVD-SiC coated C_f/SiC and SiC_f/SiC composites, despite the presence of their natural flaws, were successfully joined as in both cases, a uniform, homogenous and defect free joining interface was obtained. Backscattered SEM images of polished cross sections of CVD-SiC coated C_f/SiC samples joined with the Ti_3SiC_2 pre-sintered foil are shown in Fig. 3. The microstructural features of the cross sections of the coated SiC_f/SiC joints were identical to the coated C_f/SiC joined component.

The SEM analysis revealed several important characteristics of the behaviour of the Ti_3SiC_2 pre-sintered foil during joining. Fig. 3a shows that the Ti_3SiC_2 foil exhibited a significant ductility during joining as it bent and conformed very well to the rough surface of the CMC materials at the macro-scale (highlighted in the circles in Fig. 3a). This is not surprising as Ti_3SiC_2 is well known as a material that can show large plastic deformation at temperatures ≥ 1300°C [13, 14]. Similarly, higher

magnifications of the cross section showed that the joining filler was conformal and thus well copied the rough surface of the CVD-SiC layer at the micro-scale, resulting in a wavy character of interface. Due to this conformal behaviour of the Ti_3SiC_2 foil, no voids, cracks or any defects were observed along the CVD-SiC/Ti_3SiC_2 interface.
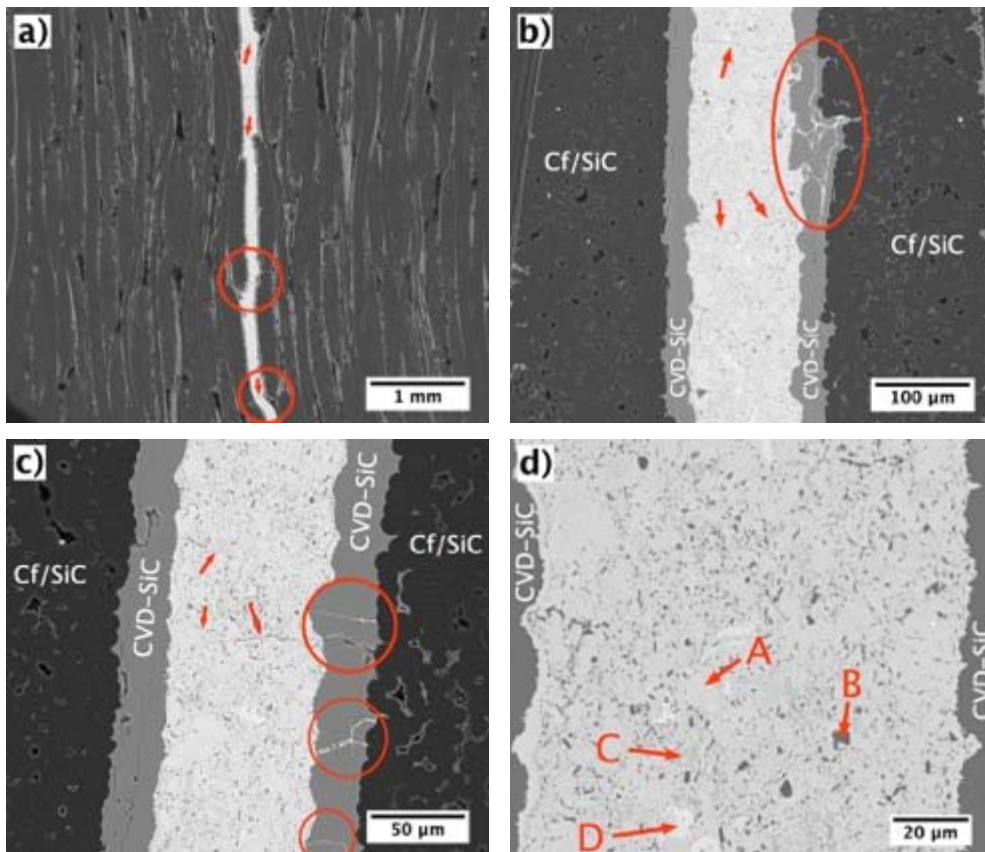

Fig. 3 Backscattered SEM images of the polished cross section of the coated C_f/SiC composites joined with Ti_3SiC_2 pre-sintered foil using SPS.

Most importantly, the Ti_3SiC_2 joining filler penetrated into the cracks in the CVD coating; effectively healing the surface cracks of the coating (highlighted by the red circles in Fig. 3b, c). It is well known that these cracks are intrinsic in the CVD-SiC layer and formed during manufacturing of CMCs due to the thermal expansion coefficient mismatch between the SiC coating and C_f/SiC substrate [1]. It can be seen that these cracks did not propagate during joining into the interlayer and therefore transverse cracks across the joining area did not form in the joined components. As

mentioned earlier, Ti_3SiC_2 shows high plastic deformation at temperatures ≥ 1300°C [13], so the joining temperature of 1300°C along with the pressure applied during joining (50 MPa) allowed the joining filler to penetrate and heal the cracks in the CVD coating. The applied temperature and external pressure enabled plastic flow of the joining material, which was pushed into the surface cracks in the CVD-SiC during joining. Therefore, the cracks that were not directly connected to the joining interlayer remained unfilled; see the cracks in the CVD coating on the left side to the interlayer in Fig. 3c. In addition, the pressure and electric current applied during SPS joining were reported to promote diffusion of the joining filler [9, 11], so the solid-state diffusion could also have contributed to the crack healing. Such a crack healing allows the joining media to integrate more with the substrate, which is believed to strengthen the joining interface.

Apart from the cracks in the CVD-SiC layer, very fine cracks were found in the joining filler in some areas, as highlighted by the arrows in Fig. 3a, b, c. Since the pre-sintered Ti_3SiC_2 foil was fully dense, no pores were found in the joining interlayer. Similar small cracks in the Ti_3SiC_2 joining interlayer were observed by Zhou et al. [10], but their presence did not deteriorate the mechanical performance of the joints. These small cracks may have formed due to the internal stresses generated and slight volume change during the cooling from the joining temperature [10, 19]. It is also worthwhile mentioning that transverse cracks were reported to cause less damage to the joining strength than cracks parallel to the joining interface [1, 18].

Fig. 3d shows the microstructure of the Ti_3SiC_2 interlayer at a higher magnification. The results of the EDS analysis of four distinct phases are shown in the supplementary information, Figure S.3. Taking both the EDS of the joining

interlayer (Figure S.3 in the supplementary material) and the XRD of the as-sintered Ti_3SiC_2 (Figure S.2 in the supplementary material) into account, it can be concluded that the Al_2O_3 particles (Fig. 3d "B") were homogenously distributed in the microstructure of Ti_3SiC_2 (Fig. 3d "A"). The Al_2O_3 particles had either plate-like or round morphologies and their size varied from several hundreds of nanometers up to 4 μm. Besides the Al_2O_3 phase, a small amount of titanium silicide was present in the microstructure, probably in both the forms of Ti_5Si_3 (light grey phase – "C" in Fig. 3d) and $TiSi_2$ (very bright areas – "D" in Fig. 3d). The presence of the titanium silicides was not detected by the XRD analysis of the pre-sintered Ti_3SiC_2 foil (Figure S.2 in the supplementary material) due to fact that its content was below the detection limit of the XRD.

It should be pointed out that the SEM analysis of the cross sections did not reveal any signs of Ti_3SiC_2 decomposition or its reaction with the CVD β-SiC coating. No obvious transition layer was found at the interface between the Ti_3SiC_2 interlayer and the CVD-SiC, as is usually observed when a reaction takes place during joining [18, 19, 11]. Moreover, the SEM/EDS analysis did not reveal any significant change in the elementary composition of the Ti_3SiC_2 filler penetrated into the CVD-SiC cracks when compared to the material in the middle of the joint.

In order to verify that neither reaction nor Ti_3SiC_2 decomposition occurred during SPS joining, micro-XRD analysis was carried out on the fracture surfaces of the joined components after the mechanical testing. The area of interest was carefully chosen to investigate the crystalline phases in the Ti_3SiC_2 interlayer that partially covered the fracture surfaces. Fig. 4 shows the micro-XRD patterns taken from the fracture surfaces of the coated SiC_f/SiC and the coated C_f/SiC joined

components. The micro-XRD analysis revealed the presence of Ti_3SiC_2 as the main crystalline phase in the interlayer. The presence of the additional SiC and C peaks is believed to come from the CMC matrix materials. No additional phases were detected by the micro-XRD of the Ti_3SiC_2 interlayer after the joining.
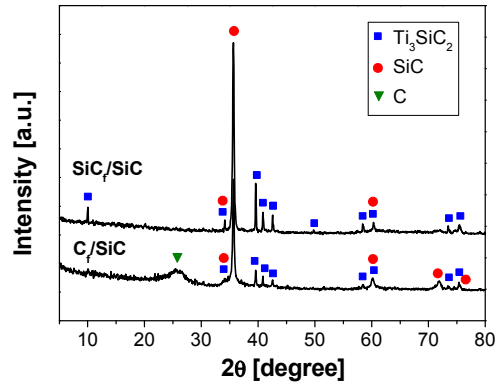

Fig. 4 Micro-XRD patterns of the Ti_3SiC_2 interlayer present on the fracture surfaces of SiC_f/SiC and C_f/SiC composites, both coated and joined with Ti_3SiC_2 interlayer using SPS.

These results are in good agreement with the work of Dong et al. [9] who did not observe any reaction or decomposition when monolithic SiC was joined with Ti_3SiC_2 powder using hot pressing at 1300°C with a holding time of 30 minutes. Once the reaction took place (above 1400°C), the amount of Ti_3SiC_2 decreased while the amount of TiC increased. They also reported the formation of $TiSi_2$ as a result of the reaction between Ti_3SiC_2 and the Si-enriched environment [9]. El-Raghy and Barsoum [20] as well as Gao et al. [21] also reported that Ti_3SiC_2 decomposes into TiC_x along with an outward diffusion and evaporation of Si in a graphite-rich environment at temperatures above 1350°C. Zhou et al. [10] found both TiC_x and Ti_xSi_y in the interlayer when SiC was joined with a Ti_3SiC_2 tape film using SPS at temperatures above 1300°C, while the Ti_3SiC_2 interlayer started decomposing from a joining temperature of 1400°C. On the other hand, Zeng et al. [22] reported that

the Ti_3SiC_2 material started to decompose after 1h at 1300°C in a furnace with graphite heating elements. They found TiC_y as the final product and $Ti_5Si_3C_x$ as the intermediate product, while Ti_xSi_y was not observed. These results show that decomposition of Ti_3SiC_2 is a complex phenomenon and is significantly affected by the external conditions, such as temperature, time, and environment. The common result of all of these works was that once the decomposition of Ti_3SiC_2 took place, the presence of TiC phase was always found as a final product after decomposition. However, no additional phase was found in the interlayer after joining process when compared to the initial pre-sintered foil, and this confirms that neither decomposition of Ti_3SiC_2 (no TiC) nor its reaction with the matrix (no $TiSi_2$) occurred during the joining.

The above observations suggest that, as intended, the joining conditions in the present work were successfully selected to prevent a reaction between the Ti_3SiC_2 interlayer and the CVD β-SiC in order to avoid damage to the protective coating on the CMCs. It can be concluded that strong, defect-free joints of the coated CMCs were obtained due to a solid-state diffusion bonding between the Ti_3SiC_2 and CVD β-SiC during SPS joining process at 1300°C and 50 MPa for 5 minutes. Since the Ti_3SiC_2 foil did not melt, shrink or react with the CVD-SiC coating on the CMCs, the final thickness of the joining interface was predetermined by the initial thickness of the Ti_3SiC_2 foil; what is another important advantage of this solid-state diffusion joining process.

3.4 Cross-section analysis of the joined CMCs without a protective CVD-SiC layer

Similar to the results for the joined CMCs coated with the CVD β-SiC, a strong bonding appeared to form between the Ti_3SiC_2 pre-sintered foil and the uncoated C_f/SiC composites. Fig. 5 shows backscattered SEM images of the polished cross section of the joined uncoated C_f/SiC with T300 1K carbon fibres. The Ti_3SiC_2 pre-sintered foil again showed a significant level of ductility as it conformed very well to the rough surface of the CMCs; avoiding pores, cracks or any defects forming along the interface. The joining interface is continuous, free of micro-defects regardless the carbon fibre orientation (parallel or perpendicular to the surface). This result shows that no specific preparation of the CMC surfaces to be joined is required before joining, contrary to the previous work where polishing of the surfaces was required to reduce the roughness and maximise the contact surface [8]. The microstructure of the interlayer was identical to the one observed in the joints of the coated CMCs; containing small amounts of the Al_2O_3 particles and titanium silicide. No other phases were found in the interlayer either by SEM/EDX or by XRD analysis.

Unlike for the joined CMCs coated with the external layer of CVD β-SiC, two distinct interfaces were observed. The first one was between the Ti_3SiC_2 interlayer and the SiC matrix while the second one was between the interlayer and the carbon fibres (in both parallel and perpendicular orientations to the surface as highlighted in Fig. 5a). Interestingly, a significant difference can be seen when these two interfaces are compared. When the Ti_3SiC_2 interlayer was in contact with carbon fibres (regardless their orientation), an additional reaction layer was found in the interlayer (highlighted by circle in Fig. 5b). The reaction layer consisted of dark grey particles, forming an almost continuous layer with a thickness of ~ 1 μm. Fig. 6

shows the results of the EDS mapping of the interface. It is clear that the reaction layer is enriched with Si while depleted in Ti. As the layer also contained carbon, it is believed that the SiC was formed at the interface as a result of the reaction between the Ti_3SiC_2 and carbon fibres. The formation of such a SiC reaction layer was also reported during the joining of C_f/C with Ti_3SiC_2 tape [11].

On the other hand, when the interlayer was in contact with the SiC matrix, no reaction layer was observed in the joining interlayer. The interface was identical to the one observed between the Ti_3SiC_2 interlayer and the CVD β-SiC in the case of joined CMCs with the protective coating. The infiltration of the joining filler into the cracks in the SiC (shown by arrows in Fig. 5b) was again observed as occurred during joining of the coated CMCs. The EDS mapping analysis did not reveal any reaction layer in the Ti_3SiC_2 filler at the interface between the Ti_3SiC_2 and SiC matrix, see Figure S.4 in the supplementary material. In good agreement with the SEM analysis of the joints of the coated C_f/SiC, even when the Ti_3SiC_2 filler penetrated into the SiC cracks, there was no sign of any reaction with the SiC.
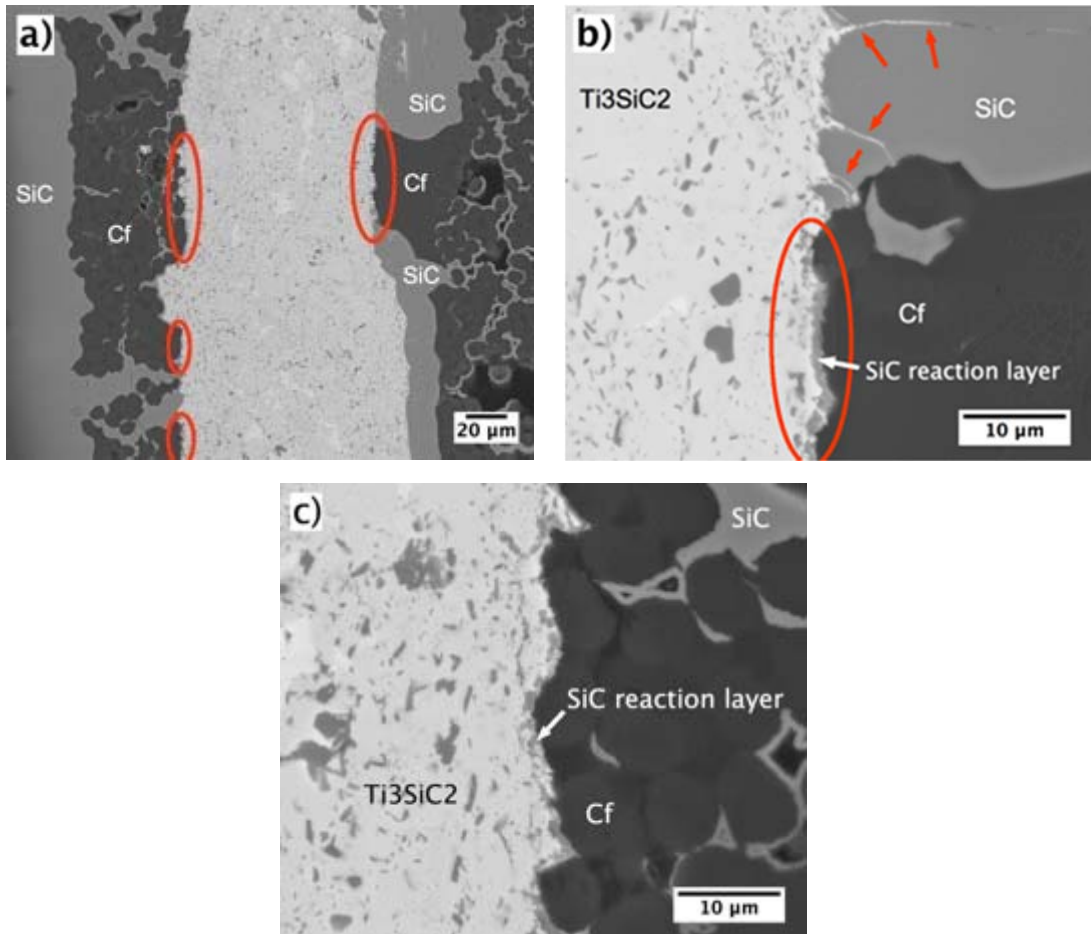
Fig. 5 Backscattered SEM images of the polished cross section of two uncoated C_f/SiC composites (T300 1K) joined with the Ti_3SiC_2 pre-sintered foil using SPS.

The infiltration of the joining filler into the inter-spaces of carbon fibres was limited because of the limited number of free interspaces of C_f near the interface (see Fig. 5a). In addition, the reaction between Ti_3SiC_2 and carbon fibres might also have inhibited the infiltration of the filler into the inter-spaces of the C_f. Once SiC formed at the interface, it acted as a barrier to inhibit further outward diffusion of Si from the filler and inward diffusion of C from the matrix [11]. Fig. 5c shows the fact that the SiC reaction layer may have acted as a barrier and inhibited the joining filler penetrating further into the composites via the interspaces between the carbon fibres. In conclusion, good, apparently strong, defect-free joints of the uncoated C_f/SiC were obtained during the SPS joining at 1300°C and 50 MPa for 5

minutes by the combination of both reactive and diffusion bonding when the Ti_3SiC_2 pre-sintered foil was in contact with C_f and SiC, respectively. It is important to point out that both reactive and diffusion bonding occurred again (as for the joining of coated CMCs) via solid state diffusion, i.e. without forming a liquid phase as neither melting nor shrinking were observed in the joints.
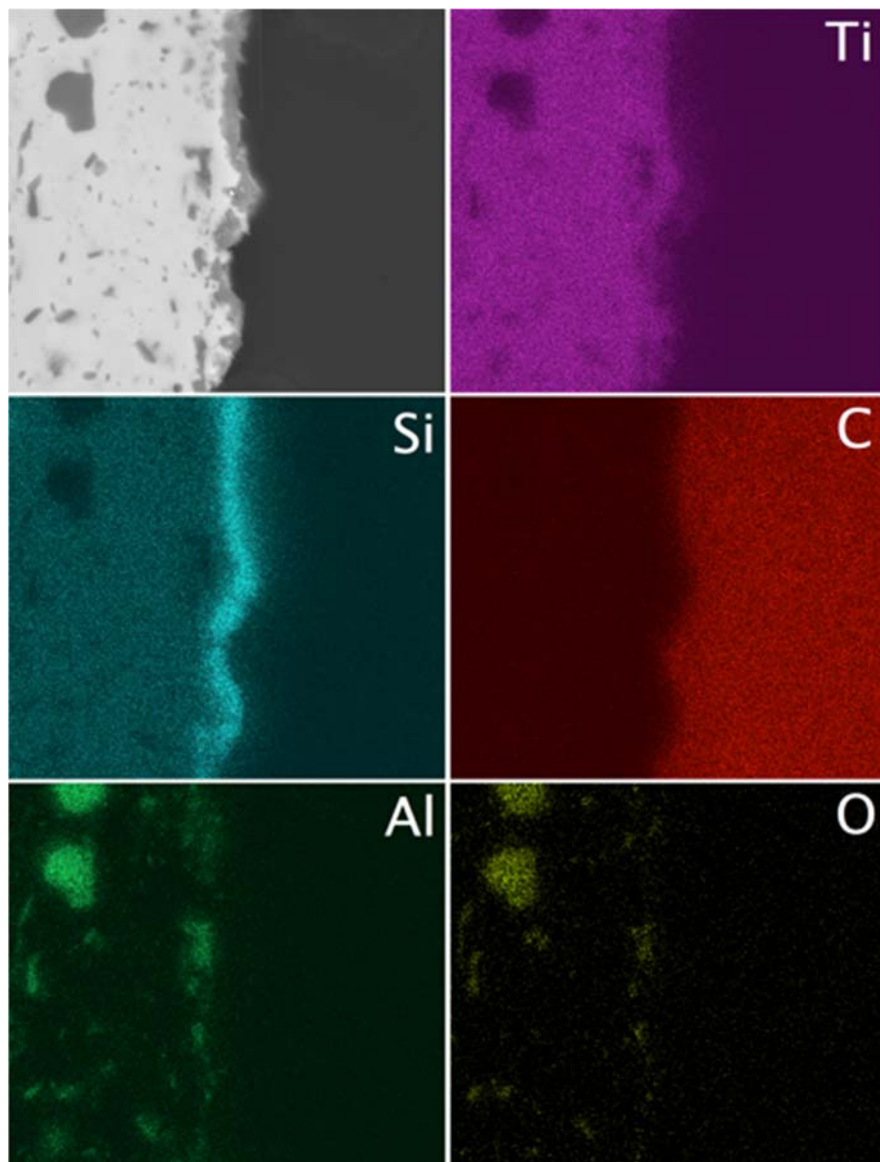

Fig. 6 EDS mapping of the elemental composition at the interface between the Ti_3SiC_2 interlayer and carbon fibres for the uncoated C_f/SiC composites (T300 1K).

As discussed above, the presence of TiC in the microstructure of Ti_3SiC_2 is always a result of Ti_3SiC_2 decomposition in a carbon-rich environment [9, 10, 11, 20, 21, 22]. However, TiC was again not found in the microstructure of the interlayer either by XRD or SEM/EDS analysis. It is therefore believed that the decomposition of Ti_3SiC_2 did not occur during joining of the uncoated CMCs similarly as it did not occur during joining of the coated CMCs in this work. This is in good agreement with the other works mentioned above that the decomposition of the Ti_3SiC_2 should not take place at temperatures ≤ 1300°C. Therefore, the SiC reactive layer was not formed as a result of the decomposition of Ti_3SiC_2 (into gaseous Si and non-stoichiometric TiC) followed by the reaction with the carbon from matrix as it occurred in [11] while joining the uncoated C_f/C composites. It is more likely that a small amount of free Si, which was reported [16] to be present in the as-synthesized Ti_3SiC_2 powder (∼ 2.6 wt.%; ∼14.4 mol.%), reacted with the carbon from the C_f/SiC matrix to form the SiC reaction layer at the interface. A small amount of free Si most probably came from the interlayer to react with carbon fibres as the uncoated C_f/SiC composites were manufactured using CVI process and did not contain any free Si.

3.5 Apparent shear strength of the joined CMC components

All of the joined CMC components were ready for the shear strength testing after SPS joining. No further machining or other sample preparation was needed as the sample misalignment was kept to a minimum during joining. Any very slight misalignment was balanced by the articulating sample grips used in the testing jig.

It must be pointed out that before the single lap offset test, the single lap test was performed on the joined CMCs, Fig. 2a. However, this test was found to be

inappropriate as delamination of the CMCs far away from the joining interface occurred during testing; see schematic crack propagation in Fig. 2a. In other words, the joining interface was stronger than the interlaminar shear strength of the CMCs, and too strong for obtaining the apparent shear strength of the joints. Since the CMC samples were not joined with any offset, before testing the Cu bars were placed on the opposite sides of the joined assembly as an artificial step to enable a single lap offset configuration (Fig. 2b). The crack propagated along and/or very close to the joining interface (as schematically shown in Fig. 2b), suggesting the apparent shear strength of the joints was obtained.
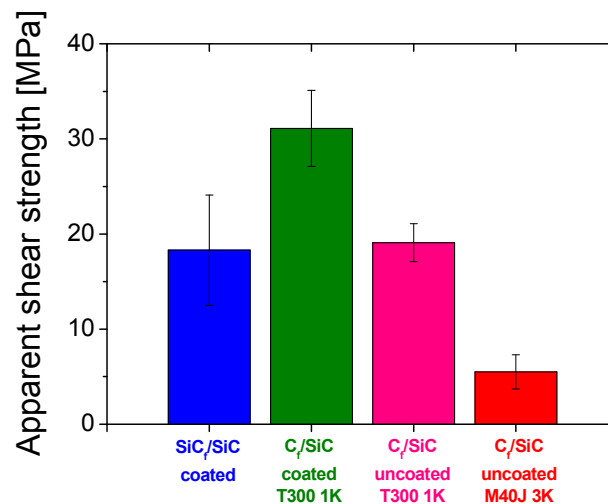

Fig. 7 Results of the single lap offset shear test for all investigated joined CMCs.

Fig. 7 shows the result of the single lap offset shear test for all four CMCs joined with the pre-sintered Ti_3SiC_2 foil using SPS. The joined C_f/SiC coated with a protective CVD β-SiC layer exhibited the best mechanical performance, as the average apparent shear strength was 31.1 ± 4.0 MPa. On the other hand, the uncoated C_f/SiC with M40J 3K carbon fibres showed the lowest shear strength (5.5 ± 1.8 MPa) among all of the investigated joined components. When compared to the

other uncoated C_f/SiC with T300 1K carbon fibres (19.1 ± 2.0 MPa), this suggests that the M40J 3K carbon fibres resulted in the lowest shear strength of the joined components. As described in the supplementary material S.5, M40J 3K fibres are much stiffer than T300 1K fibres and this stiff fabric structure had a tendency to spring back during the gradient CVI process, leading to separation of the fabric layers. Therefore, bigger voids between the fabric layers were found when the stiffer M40J 3K fibres were used (see Figure S.1 in the supplementary material). These separate fabric layers resulted in poor mechanical performance of the joined uncoated C_f/SiC components with M40J 3K carbon fibres. This was further confirmed by the fracture surface analysis after the single lap offset shear tests. Fig. 8 shows a macro view of the fracture surfaces of all of the investigated joined CMCs. While the three other joined CMC samples always delaminated at, or very close to the joining interface, the uncoated C_f/SiC with M40J carbon fibres samples always delaminated in the composite, far away from the joining interface (as schematically shown in Fig. 2a). Fig. 8d shows that the joined couple did not fail in the middle, but one half of the joined component was much thicker than the other one after the failure. The pre-sintered foil was far beneath the fracture surface on one part of the composite (right hand part in Fig. 8d). This is consistent with the relatively poor mechanical properties of this type of CMC, as the joint was much stronger than the shear strength between the individual fabric layers of the composite.
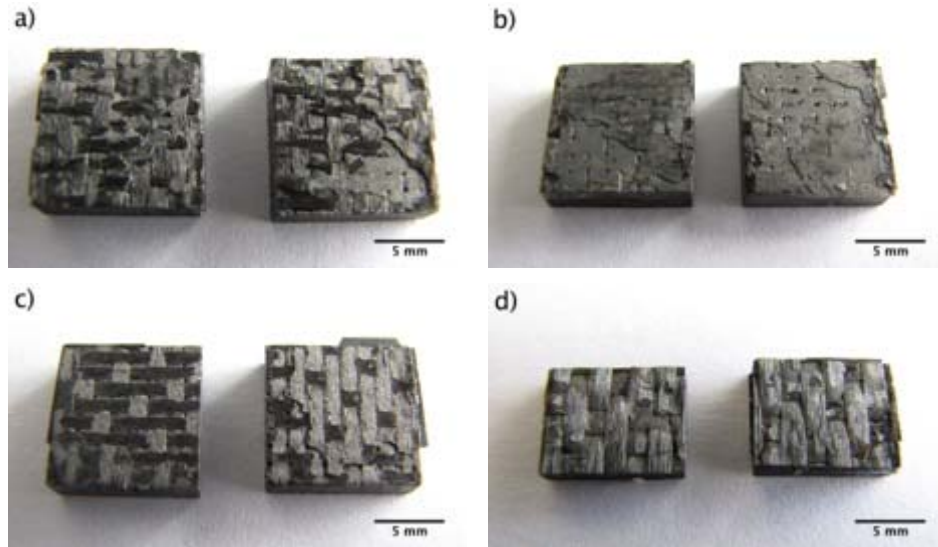
Fig. 8 Macro images of the fracture surfaces of all joined CMCs after the single lap offset shear test: a) coated SiC_f/SiC; b) coated C_f/SiC; c) uncoated C_f/SiC made of T300 1K fibres; d) uncoated C_f/SiC made of M40J 3K fibres.

For the other three joined composites the crack propagated by a combination of two different modes: i) along the joining interface, and ii) through the composite near the interface; as schematically shown in Fig. 2b. Crack propagation through the interlayer leading to the delamination within the pre-sintered foil was not observed whatsoever. Therefore, the apparent shear strength of the joined components was influenced by both the strength of the interface and the shear strength of the composites.

The results of the apparent shear strength test in Fig. 7 also show that the shear strength of the joined couple of the uncoated C_f/SiC was lower (19.1 ± 2.0 MPa) than that of the CVD-SiC coated C_f/SiC (31.1 ± 4.0 MPa). In the case of coated C_f/SiC, the infiltration of the joining filler into the surface cracks in the CVD-SiC coating allowed the filler to be more uniformly integrated with the matrix all along the interface. This resulted in a higher shear strength than that of the uncoated joined samples. On the other hand, two significantly different interfaces (infiltration

of the filler into the cracks in SiC matrix, while formation of the SiC reaction layer when in contact with carbon fibres) rather than a uniform interface may have led to the lower shear strength of the uncoated joined components. The joining filler was not that well integrated with the CMCs as the number of cracks in SiC matrix healed with the Ti_3SiC_2 filler was limited and much lower than in the case of the external CVD-SiC coating. Moreover, the infiltration of the filler into the interspaces of C_f was only partially observed (Fig. 5c) due to a lack of free interspace of the C_f at the interface and the reaction between the Ti_3SiC_2 interlayer and carbon fibres. Therefore, a positive effect of the reaction bonding in the uncoated C_f/SiC on the shear strength of the joined components was not observed in the present work.
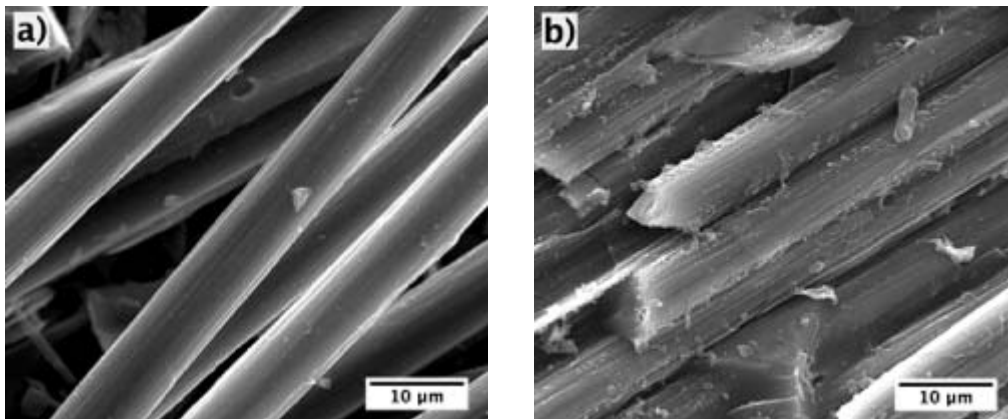

Fig. 9 SEM images of the details of SiC Tyranno fibres on the fracture surfaces of: a) as-received coated SiC$_f$/SiC composites; b) joined couple of coated SiC$_f$/SiC.

According to the CMCs supplier (MT Aerospace), the shear strength of the as-received SiC$_f$/SiC and C$_f$/SiC composites is 35 – 50 MPa and 25 -35 MPa, respectively. The average value of shear strength of the joined couple of the coated C$_f$/SiC measured in this work (31.1 ± 4.0 MPa) is similar to the shear strength of the as-received composites. However, the apparent shear strength of the joined couple of the coated SiC$_f$/SiC was significantly lower (18.3 ± 5.8 MPa) than that of the as-

received composites. Fig. 9 shows the SEM images of the SiC Tyranno S-type fibres observed on the fracture surfaces of the as-received coated SiC_f/SiC and the joined coated SiC_f/SiC composites, respectively. While in both cases the SiC_f fibres are detached from the SiC matrix, degradation of the Tyranno SiC fibres is obvious on the fracture surface of the joined couple (Fig. 9b). This clearly confirms that despite the external SiC protective coating on the SiC_f/SiC composites, the joining conditions used in the present work (SPS, 1300°C and 50 MPa) were too extreme for the SiC fibres. The degradation of a variety of SiC fibres at temperatures above 1000-1200°C was often reported in the literature [23, 24, 25]. Since degradation of SiC fibres is strongly affected by temperature, time and atmosphere [24, 25], the external pressure (50 MPa) applied during the SPS joining at 1300°C most probably accelerated the process of degradation. This degradation of the SiC fibres resulted in the deterioration of the apparent shear strength of the investigated joints of the CVD-SiC coated SiC_f/SiC composites.

Although the cracks propagated in a mixed mode (along the interface, and/or through the composite) in both cases, a small difference can be seen when the backscattered SEM images of the fracture surfaces of the coated SiC_f/SiC and the coated C_f/SiC are compared, Fig. 10. In the case of coated SiC_f/SiC, the crack propagated through the one part of the composite and before growing into the other part through the interlayer, the crack propagated for a short distance along the CVD-SiC/Ti_3SiC_2 interface (Fig. 10a). On the other hand, when a crack propagated from one part of the C_f/SiC into other part, the crack path along the CVD-SiC/Ti_3SiC_2 interface was significantly larger than it was for the coated SiC_f/SiC (Fig. 10b). This led to delamination of a significant part of the joining foil from the CVD-SiC surface.

In addition, cracks also propagated partially along the interface between the CMC and the CVD-SiC coating. The possible crack paths during single lap offset shear test of different joined CMC components are schematically shown in Figure S.5 in the supplementary material. All of this confirms that the matrix of SiC_f/SiC was significantly weaker than that of the C_f/SiC, as it was energetically more favourable for a crack to propagate through the SiC_f/SiC composite in proximity of the interface rather than along the interface. More importantly, since the crack propagated mainly along the CVD-SiC/Ti_3SiC_2, the apparent shear strength of the joints of coated C_f/SiC composites (31.1 ± 4.0 MPa) was probably very close to the "pure" shear strength of the CVD-SiC/Ti_3SiC_2 interface.
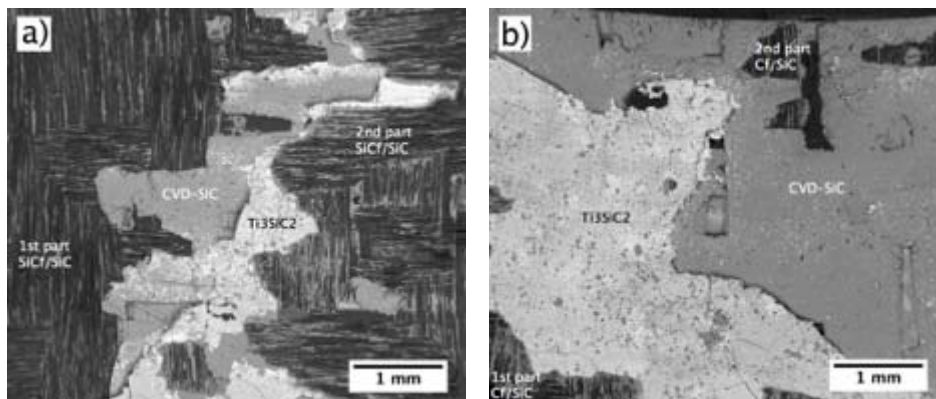

Fig. 10 Backscattered SEM images of the fracture surfaces of joined CMCs components after single lap offset shear test: a) coated SiC_f/SiC; b) coated C_f/SiC.

Conclusions

Four different types of CMCs (coated SiC_f/SiC, coated C_f/SiC and two types of uncoated C_f/SiC with different carbon fibres) were successfully joined to their counterparts with a pre-sintered Ti_3SiC_2 foil using SPS technology at a temperature of 1300°C, an external pressure of 50 MPa, with a dwell time of 5 minutes. For the first time pre-sintered Ti_3SiC_2 foil rather than the Ti_3SiC_2 powder or Ti_3SiC_2 tape was used as a joining filler. The pre-sintered foil and the joining parameters were

carefully selected to avoid the decomposition of Ti_3SiC_2 and the reaction between the joining filler and the CVD coating, which would have deteriorated the oxidation protective function of the coating.

The joints of the CVD-SiC coated C_f/SiC and SiC_f/SiC composites were produced by solid-state diffusion bonding between the Ti_3SiC_2 interlayer and the CVD β-SiC layer. No reaction between the Ti_3SiC_2 and CVD-SiC was observed. The pre-sintered Ti_3SiC_2 foil showed a significant level of ductility during joining as it conformed very well to the rough surface of the CMCs and/or CVD coating at both the macro- and micro-scales. The infiltration of the joining filler into the surface cracks in the CVD β-SiC coating allowed filler to be more uniformly integrated with the matrix material all along the interface. Since the Ti_3SiC_2 foil did not melt, shrink or react with the CVD-SiC coating on the CMCs, the final thickness of the joining interface was predetermined by the initial thickness of the Ti_3SiC_2 foil; what is another important advantage of this diffusion joining process. The apparent shear strength of the joined coated C_f/SiC was 31.1 ± 4.0 MPa. This value is close to the shear strength of the CVD-SiC/Ti_3SiC_2 interface, as the main crack path was along the interface rather than through the composites in proximity of the interface.

Despite the protective CVD β-SiC coating, the degradation of SiC fibres reduced the apparent shear strength of the joints (18.3 ± 5.8 MPa). The external pressure applied during the SPS joining most probably accelerated the degradation of the SiC fibres.

A combination of both reaction and diffusion bonding was observed when the uncoated C_f/SiC composites were joined. Both types of bonding occurred via solid-state diffusion, i.e. without presence of a liquid phase as the MAX phase did not

melt during joining. The formation of SiC reaction layer in the joining interlayer was observed at the interface between the carbon fibres and the Ti_3SiC_2 interlayer. When in contact with the SiC matrix, the Ti_3SiC_2 joining filler infiltrated into the cracks in the SiC at the interface, and no reaction between the two phases was found. The apparent shear strength of the joined uncoated C_f/SiC with T300 1K carbon fibres was found to be 19.1 ± 2.0 MPa. The combination of both diffusion and reaction bonding produced the lower shear strength when compared to when only diffusion bonding occurred in the joining of the coated CMCs. The stiffer M40J 3K carbon fibres showed a tendency to spring back during the gradient CVI process, forming big voids between the individual fabric layers. This was the reason for the significantly lower apparent shear strength of the joined uncoated C_f/SiC with the M40J 3K carbon fibres (5.5 ± 1.8 MPa).

Acknowledgement

References

1. S. Rizzo, S. Grasso, M. Salvo, V. Casalegno, M.J. Reece, M. Ferraris, Joining of C/SiC composites by spark plasma sintering, J. Eur. Cer. Soc. 34 (2014) 903-913.

2. C. Jiménez, K. Mergia, M. Lagos, P. Yialouris, I. Agote, V. Liedtke, S. Messoloras, Y. Panayiotatos, E. Padovano, C. Badini, C. Wilhelmi, J. Barcena, Joining of ceramic matrix composites to high temperature ceramics for thermal protection systems, J. Eur. Cer. Soc. 36 (2016) 443-449.

3. M. Salvo, S. Rizzo, V. Casalegno, K. Handrick, M. Ferraris, Shear and bending strength of SiC/SiC joined by a modified commercial adhesive, Inter. J. Appl. Ceram. Tech. 9 (2012) 778-785.

4. Y. Katoh, L.L. Snead, T. Chenga, C. Shih, W.D. Lewis, T. Koyanagi, T. Hinoki, C.H. Henager Jr., M. Ferraris, Radiation-tolerant joining technologies for silicon carbide ceramics and composites, J. Nucl. Mater. 448 (2014) 497-511.

5. M. Ferraris, M. Salvo, V. Casalegno, A. Ciampichetti, F. Smeacetto, M. Zucchetti, Joining machined SiC/SiC composites for thermonuclear fusion reactors, J. Nucl. Mater. 375 (2008) 410-5.

6. P. Colombo, B. Riccardi, A. Donato, G. Scarinci, Joining of SiC/SiC$_f$ ceramic matrix composites for fusion reactor blanket applications, J. Nucl. Mater. 278 (2000) 127-135.

7. R. S. Kumar, Analysis of coupled ply damage and delamination failure processes in ceramic matrix composites, Acta Mater. 61 (2013) 3535-3548.

8. S. Grasso, P. Tatarko, S. Rizzo, C. Hu, Y. Katoh, M. Salvo, M.J. Reece, M. Ferraris, Joining of β-SiC by spark plasma sintering, J. Eur. Ceram. Soc. 34 (2014) 1681-1686.

9. H. Dong, S. Li, Y. Teng, W. Ma, Joining of SiC ceramic-based materials with ternary carbide Ti_3SiC_2, Mat. Sci. Eng. B 176 (2011) 60-64.

10. X. Zhou, Y.H. Han, X. Shen, S. Du, J. Lee, Q. Huang: Fast joining SiC ceramics with Ti_3SiC_2 tape film by electric field-assisted sintering technology, J. Nucl. Mater. 466 (2015) 322-327.

11. X. Zhou, H. Yang, F. Chen, Y.-H. Han, J. Lee, S. Du, Q. Huang, Joining of carbon fiber reinforced carbon composites with Ti_3SiC_2 tape film by electric field assisted sintering technique, Carbon 102 (2016) 106-115.

12. M.W. Barsoum, The $M_{N+1}AX_N$ phase: A new class of solids; Thermodynamically stable nanolaminates, Prog. Solid. State Chem. 28 (2000) 201-281.

13. T. El-Raghy, M.W. Barsoum, A. Zavaliangos, S.R. Kalidindi, Processing and mechanical properties of Ti_3SiC_2: II, Effect of grain size and deformation teperature, J. Am. Ceram. Soc. 82[10] (1999) 2855-2860.

14. M. Radovic, M.W. Barsoum, T. El-Raghy, J. Seidensticker, S. Wiederhorn, Tensile properties of Ti_3SiC_2 in the 25-1300°C temperature range, Acta Mater. 48 [2] (2000) 453-459.

15. F. Li, H. Zhang, Q. Wang, D. Qu, T. Zhou, B. Kim, Y. Sakka, C. Hu, Q. Huang, Microwave sintering of $Ti_3Si(Al)C_2$ ceramic, J. Am. Ceram. Soc. 97[9] (2014) 2731-2735.

16. K. Sato, M. Mishra, H. Hirano, C. Hu, Y. Sakka, Pressureless sintering and reaction mechanism of Ti$_3$SiC$_2$ ceramics, J. Am. Ceram. Soc. 97[5] (2014) 1407-1412.

17. H.B. Zhang, Y.C. Zhou, Y.W. Bao, M.S. Li, Improving the oxidation resistance of Ti$_3$SiC$_2$ by forming a Ti$_3$Si0.9Al10.1C$_2$ solid solution, Acta Mater. 52 (2004) 3631-3637.

18. F. Lan, K. Li, H. Li, L. Guo, Y. He, L. Zhang, High-temperature property of carbon/carbon composite joints bonded with ternary Ti-Si-C compound, J. Alloy Comp. 480 (2009) 747-749.

19. J. Wang, K. Li, W. Li, H. Li, Z. Li, L. Guo, The preparation and mechanical properties of carbon/carbon composite joints using Ti-Si-SiC-C filler as interlayer, Mat. Sci. Eng. A 574 (2013) 37-45.

20. T. El-Raghy, M.W. Barsoum, Diffusion kinetics of the carburization and silicidation of Ti$_3$SiC$_2$, J. Appl. Phys. 83[1] (1998) 112-119.

21. N.F. Gao, Y. Miyamoto, D. Zhang, On physical and thermomechanical properties of high-purity Ti$_3$SiC$_2$, Mater. Lett. 55 (2002) 61-66.

22. J. Zeng, S. Ren, J. Lu, Phase evolution of Ti$_3$SiC$_2$ annealing in vacuum at elevated temperatures, Int. J. Appl. Ceram. Technol. 10[3] (2013) 527-539.

23. M. Ferraris, M. Montorsi, M. Salvo, Glass coating for SiC$_f$/SiC composites for high-temperature application, Acta Mater. 48 [18-19] (2000) 4721-4724.

24. J. LLorca, M. Elices, J.A. Celemin, Toughness and microstructural degradation at high temperature in SiC fiber-reinforced ceramics, Acta Mater. 46 [7] (1998) 2441-2453.

25. J. Ramírez-Rico, J. Martínez-Fernández, M. Singh, Effect of oxidation on the compressive strength of sintered SiC-fiber bonded ceramics, Mat. Sci. Eng. A 534 (2012) 394-399.